Electron Capture by the Image Charge of a Metal Nanoparticle

V. Kasperovich, K. Wong, G. Tikhonov, and V. V. Kresin
Department of Physics and Astronomy, University of Southern California, Los Angeles, California 90089-0484
(Received 6 June 2000)

We have measured absolute cross sections for the capture of low-energy electrons by large free sodium nanoclusters ($\sim 10^4$ atoms, or 4 nm radius). To explain the results, it is necessary to go beyond the commonly used induced-dipole approximation and to employ the full image-charge interaction potential which accounts for the finite size of the particle. This potential yields an exact analytical expression for the capture cross section and leads to good agreement with the data. It is suggested that electron capture may provide a useful tool for size characterization of nanoparticle beams.

PACS numbers: 36.40.Wa, 34.80.Ht, 61.46.+w

Experiments on free nanometer-sized metal cluster particles make it possible to apply the arsenal of molecular beam tools to systems which are at the core of nanomaterial and nanodevice research (see the reviews in [1,2] and references therein). At the same time, such experiments permit a systematic exploration of how fundamental molecular interactions extrapolate into the domain of large particles.

Metal clusters are highly polarizable, which results in the appearance of strong long-range forces [3]. In particular, an electron approaching a cluster will polarize it and, as a result, experience an attractive polarization potential $V_{\rm pol}$. In fact, it may even become captured by $V_{\rm pol}$. In a classical picture, the electron is attracted by its own image charge and, if approaching the cluster with an impact parameter smaller than a certain critical value, will spiral into the center of force.

The leading interaction term is that of a point charge with an induced dipole:

$$V_{\rm pol} = -\alpha e^2/(2r^4), \tag{1}$$

where α is the electric dipole polarizability of the cluster (for an ideal conducting sphere, $\alpha = R^3$). The corresponding classical capture cross section, known as the Langevin cross section, is given by

$$\sigma_L = (2\pi^2 \alpha e^2/E)^{1/2}, \tag{2}$$

where E is the energy of the incoming electron [4,5]. The quantum mechanical cross section [6] deviates from this result by no more than a few percent down to meV collision energies. The forms (1) and (2) have been extensively used to analyze molecular collisions with electrons and ions [7–9]; it was recently shown that the polarization potential also contributes to electron attachment to C_{60} fullerenes (see, e.g., [10]).

For strongly polarizable clusters and slow electrons, this picture promises large capture cross sections. Indeed, negative ions are readily formed in low-energy electron collisions with medium-sized sodium clusters Na_n ($n \approx 20-100$), with total cross sections [11] and anion yield curves [12] in very good agreement with Eq. (2).

Note, however, that the point-dipole potential (1) represents only the far-field component of the polarization field. What happens if the scatterer is so large that higher-order terms become significant? We describe an experiment on electron capture by sodium nanoclusters ($n \sim 10^4$ atoms, $R \approx 4$ nm) in which the finite size of the particle turns out to make a crucial contribution. In addition, we show that a measurement of this contribution directly furnishes the dimension of the particle, which is difficult to characterize by other methods in this mass range.

An outline of the experiment is shown in Fig. 1. The apparatus and the procedure used to measure attachment cross sections have been described previously [11]. To produce a beam of neutral sodium nanoparticles we have installed a vapor condensation source similar to the "smoke source" described in Ref. [13]. The beam passes through the scattering region of an electron gun consisting of a planar dispenser cathode and a set of precision grids and masks, based on the geometry of Ref. [14]. Here some of the particles may capture an electron and become negatively charged. These negative ions are pushed out of the

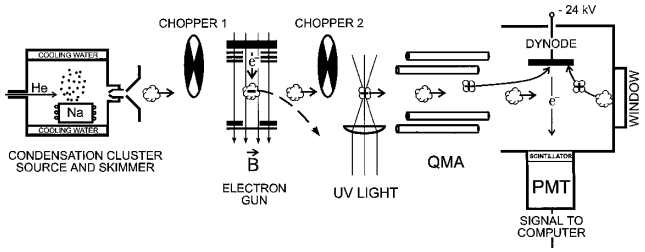

FIG. 1. Outline of the experimental arrangement (not to scale). A beam of neutral sodium nanoclusters is produced by a vapor condensation source ($T_{\rm oven} = 380$ °C, $T_{\rm nozzle} = 100$ °C, $d_{\rm nozzle} = 2$ mm, $P_{\rm He} = 1.8$ torr). Following a 1 m long free flight, the beam enters the collision region of the electron gun. Particles which capture an electron are swept away by a strong magnetic field. The remaining neutral particles continue for another 50 cm towards the beam detector, where they are fragmented and ionized by focused UV light or by surface impact (see text for details) and counted by an ion detector. Interaction cross sections are found by measuring the electron-induced beam depletion. Two high-speed chopper wheels are used to measure the velocity profile.

original beam by the 1.4 kG magnetic field which is applied to the electron gun in order to prevent dispersal of the electron ribbon by space-charge effects. The remaining neutral nanoclusters continue on to the beam detection region. The inelastic collision cross section is determined by pulsing the electron beam on and off and measuring the magnitude of beam depletion (see below).

Some comments are in order regarding the beam detection process. The particle detector in our apparatus was originally designed to study clusters ranging up to a few hundred atoms in size. It consists of an ionizing region where the beam is illuminated by near-UV light from an arc discharge lamp, a quadrupole mass analyzer (QMA), and a Daly ion counter incorporating a conversion dynode, a scintillator, and a photomultiplier tube [15]. The nanoparticle mass in the present experiment exceeds the QMA mass capacity by almost 2 orders of magnitude, but we have found two complementary counting modes which gave a signal proportional to the particle beam intensity. First, we discovered that even with the UV lamp turned off, a signal rate on the order of 10^3–10^4 counts per second was still observed. We identified it as originating from positive fragments formed upon the impact of large neutral clusters onto the glass window located just downstream of the dynode (see Fig. 1). Such processes have been described in hyperthermal surface scattering of large molecules and molecular clusters (see, e.g., [16,17]); we are currently investigating surface ionization of metal nanoparticles in more detail. The second detection mode derives from the observation that UV illumination of the nanocluster beam produced an even more abundant flux of heavy charged fragments. The QMA could not resolve their masses, but it was able to filter them out of the beam, permitting us to separate these ions from those formed by surface impact. Thus we used the "surface-ionization" and "UV-ionization" counting rates separately in order to derive two independent values for the average electron capture cross section.

As mentioned above, the cross sections were obtained by the beam depletion technique. The electron current was pulsed on and off at a rate of 4.77 Hz and the detector counting rate was recorded by a synchronized multichannel scaler. For each electron energy setting, the on/off data were collected for a 2–3 min interval. The corresponding beam depletion ratio $\Delta N/N$ was in the range of 10%–30%, reflecting the huge capture cross sections: for comparison, in an experiment with smaller ($n < 100$) clusters [11], the depletion ratio was less than 1% and data acquisition intervals of up to one hour were required.

The total effective electron-cluster interaction cross section σ_{eff} is found from $\Delta N/N = \sigma_{\text{eff}} I_{\text{el}}/(v_{\text{cl}} h)$ [18,19]. I_{el} is the electron number current, h is the height of the overlapping electron and cluster beams, and v_{cl} is the cluster beam velocity. Here σ_{eff} represents the intrinsic interaction cross section $\sigma(E)$ convoluted with the electron energy distribution $f(E - E_0)$ inherent to the electron gun, where E_0 is the nominal electron energy, i.e., the potential of the scattering region. A retarding potential technique is used to extract both the electron gun energy spread and the contact potential contribution to the nominal electron energy. The energy distribution $f(E - E_0)$ is well represented by Gaussian shape with a full width at half maximum (FWHM) of about 0.3 eV for $E_0 \leq 1$ and 0.4 eV for higher electron energies. The values for E_0 are determined to an accuracy better than 0.1 eV. The energy of the collision is appropriately represented in terms of the "adjusted electron energy" $\langle E \rangle$ which is also given by a convolution of E with $f(E - E_0)$ with an appropriate cutoff at $E = 0$ [20]. This procedure is described in more detail in Ref. [12]. Calculations showed that $\langle E \rangle \approx E_0$ already for energies of 0.5 eV and higher.

The particle beam velocity was measured with the aid of two identical choppers as indicated in Fig. 1. The velocity distribution peaks at 230 m/s with a FWHM of 20 m/s. It is interesting that the nanocluster beam, while slow, displays a narrow velocity spread similar to that of a supersonic source.

We now come to the experimental results. Figure 2 shows the total depletion cross sections σ_{eff} for electron collisions with sodium particles in the 0–7 eV energy range. The two panels correspond to the different beam detection techniques described above. The very magnitudes of the cross sections are noteworthy.

The two sets of data differ slightly in magnitude, which can be understood as follows. The condensation source produces sodium droplets with a certain size distribution. The efficiencies of the two different ionization modes are likely to have different mass dependencies and therefore amplify somewhat different portions of the size distribution. In other words, the measured cross sections are convolutions of the real size dependent $\sigma(n, E)$ with the beam mass profile and the sensitivity functions of the ionization modes. It is important to note, though, that the average particle sizes fitted to the two distributions (see below) agree to within 20%, which supports the validity of the technique.

The scattering cross section rises sharply as the electron energy goes to zero, which is a signature of electron capture and negative ion production. At first glance, the shape appears similar to that found for smaller clusters [11,12] where Eq. (2) gave a very good description of the data. However, an attempt to fit the low-energy data in Fig. 2 with such an equation fails completely. The figure shows that the curvature of the data at low energies cannot be matched by an $E^{-1/2}$ line. Clearly, the conventional treatment based on an induced point dipole picture fails for scatterers as large as those encountered here. Let us see whether the situation can be improved by accounting for the finite particle size.

We need to write down the interaction potential between an electron and a relatively large polarizable particle. It is known that surface electron spillout enhances the dipole

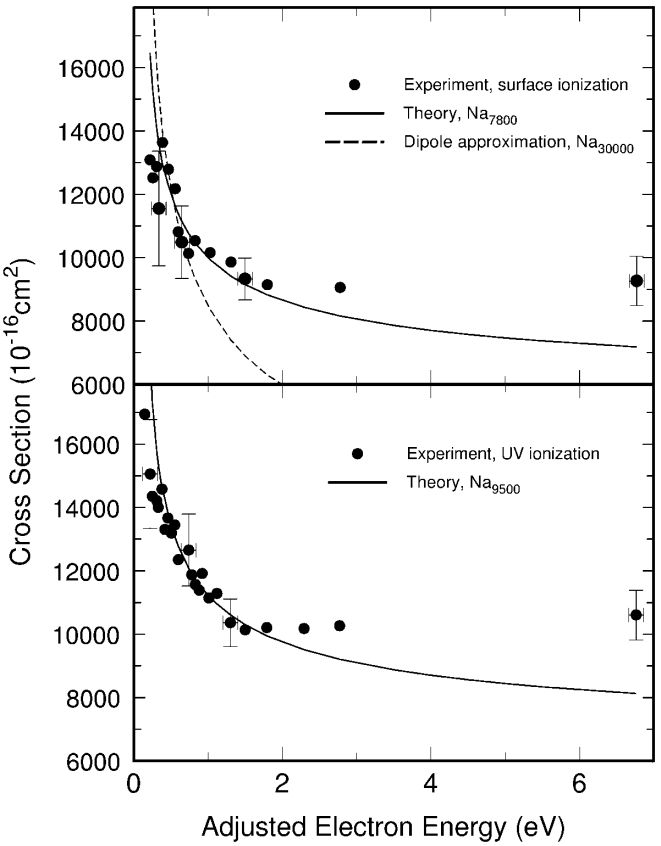

FIG. 2. Total cross sections for electron collisions with sodium nanoclusters. The upper panel shows results obtained in the surface-ionization beam detection mode and the lower panel is for the UV-ionization mode (see text). Solid lines: Image-charge capture cross sections, Eq. (4), convoluted with the electron gun resolution function. The two detection modes yield consistent results for the average particle size in the beam, $n \approx 7800$ and $n \approx 9500$, respectively ($R \approx 4$ nm). Deviations observed at higher collision energies are interpreted as the onset of direct cluster fragmentation. Dashed line: Best fit to the data using the Langevin form, Eq. (2). The poor match of the curvature and the unreasonably large particle size required by the fit (note that the geometrical cross section of $Na_{30\,000} \approx 14\,000$ Å^2) demonstrate that the dipole approximation is inadequate.

polarizability of smaller metal clusters over the value R^3 for a conducting sphere of radius R [21]. However, this correction decays with particle size and should become insignificant for the sizes dealt with here. It is therefore natural to make use of the full classical image-charge potential for the attraction between a point charge and an isolated conducting sphere of radius R [22]:

$$U = -e^2R^3/[2r^2(r^2 - R^2)]. \quad (3)$$

Equation (1) is the dipole approximation to this full expression and holds only for $r \gg R$.

Now we need to calculate the energy-dependent capture cross section for an electron spiraling in the field (3). Quantum mechanically, this is undoubtedly a challenging problem. However, as mentioned above, the full quantum solution for the dipole potential (1) gave a result which coincided, down to very low energies, with that found from classical mechanics [6]. It is therefore reasonable to expect that the classical capture cross section for U should serve well in the present case.

The recipe for calculating this cross section is given, e.g., by Landau and Lifshitz [5]. One writes down the effective potential energy $U_{\text{eff}} = U + mb^2v_\infty^2/(2r^2)$, where the second term is the centrifugal barrier (b is the electron impact parameter and v_∞ is the electron velocity at large separation). For a given kinetic energy of collision $E = mv_\infty^2/2$, there is a critical impact parameter, b_0, below which the electron can overcome the hump of U_{eff} and "fall to the center." The capture cross section is then given by $\sigma(E) = \pi b_0^2$. This procedure is simple for a power-law potential such as Eq. (1), but it turns out that even for the complete potential in Eq. (3) an exact analytical solution can be found. This was in fact pointed out by Klots [23] a few years ago. One finds the following remarkably simple result:

$$\sigma(E) = \pi R^2 + (2\pi^2\alpha e^2/E)^{1/2}. \quad (4)$$

Note that this is just a sum of the hard-sphere area of the particle and the Langevin cross section, Eq. (2).

We now try to fit the low-energy scattering data with the form (4). As Fig. 2 demonstrates, a good match is obtained. Note that the particle radius R is the only adjustable parameter. We find a satisfactory fit with $n \approx 7800$ atoms in the surface-ionization detection mode, and $n \approx 9500$ atoms in the UV-ionization mode [24,25]. These values are indeed sufficiently close to each other to support the consistency of the method. The corresponding particle radius is $R = 4.2$–4.5 nm.

Finally, we point out that, in addition to demonstrating strong image-charge attraction between electrons and nanoparticles, this measurement serves as a tool for calibrating the average nanocluster size. Beams of metal particles in this size range are of interest for basic research and for potential applications such as film deposition and materials synthesis [1]; thus it is important to be able to characterize them. There exist a number of established size calibration techniques, but each one has certain limitations.

Time-of-flight (TOF) mass spectrometry is a powerful tool with high-mass capabilities, but it is well known that the photoionization step can lead to extensive fragmentation of fragile species, including metallic particles (see, e.g., an example in Refs. [26,27]). We have measured a TOF spectrum of our beam in a 1 m long linear flight geometry with ionization by 355 nm pulses from a Nd-YAG laser (0.1–8 mJ per 5 ns pulse) and ion detection by a channeltron with a stainless steel conversion dynode. The tail of the mass spectrum indeed extended into the 2×10^5 dalton mass range ($\sim Na_{9000}$), but it was obvious that even at relatively low laser power the picture was dominated by fragmentation products. Furthermore, the detection of high masses was strongly suppressed by their inefficient secondary electron emission at the dynode, a feature well

known in mass spectrometry [28]. Note that the beam detection modes employed in our electron attachment measurement are not strongly susceptible to such biases.

Other size analysis methods include direct imaging of surface-deposited nanoclusters (a highly complex procedure which also involves the possibility of cluster fragmentation upon landing), and light scattering and absorption (see, e.g., [29–32]). It appears that the electron-attachment procedure described here may be a useful complementary technique, given the simple scaling of the cross section with particle radius and the absence of a strong bias against high masses.

In summary, we have studied the attachment of slow electrons to a beam of sodium nanoclusters containing $\sim$7000–9000 atoms (4 nm radius) produced in a vapor condensation source. Extremely large capture cross sections ($>10^4$ Å^2) were observed. To explain their behavior, it was necessary to go beyond the usual induced-dipole approximation for the attractive interaction. By taking into account the full electron-particle image charge potential (which yields an exact analytical solution for the capture cross section), we obtained very good agreement with the low-energy behavior of the data. It appears that this may be a convenient technique for calibrating the sizes of nanoparticles in beams over a wide mass range.

We are grateful to K. H. Bowen for valuable advice concerning the construction and operation of the condensation source and to W. C. Lineberger and M. Olshanii for useful discussions. This work was supported by NSF Grant No. PHY-9600039.

[1] P. Milani and S. Iannotta, *Cluster Beam Synthesis of Nanostructured Materials* (Springer, Berlin, 1999).
[2] *Clusters of Atoms and Molecules II,* edited by H. Haberland (Springer, Berlin, 1994).
[3] V. V. Kresin and C. Guet, Philos. Mag. B **79**, 1401 (1999).
[4] P. Langevin, Ann. Chim. Phys. **5**, 245 (1905).
[5] L. D. Landau and E. M. Lifshitz, *Mechanics* (Pergamon, Oxford, 1976), 3rd ed., Sec. 18.
[6] E. Vogt and G. H. Wannier, Phys. Rev. **95**, 1190 (1954).
[7] E. W. McDaniel, *Collision Phenomena in Ionized Gases* (Wiley, New York, 1964).
[8] E. W. McDaniel, *Atomic Collisions: Electron and Photon Projectiles* (Wiley, New York, 1989).
[9] A. Henglein, in *Physical Chemistry—An Advanced Treatise,* edited by W. Jost (Academic, New York, 1975), Vol. VIB.
[10] D. Klar *et al.,* Z. Phys. D **31**, 235 (1994).
[11] V. Kasperovich *et al.,* Phys. Rev. A **60**, 3071 (1999).
[12] V. Kasperovich *et al.,* Phys. Rev. A (to be published).
[13] K. M. McHugh *et al.,* Z. Phys. D **12**, 3 (1989).
[14] R. E. Collins *et al.,* Rev. Sci. Instrum. **41**, 1403 (1970).
[15] W. A. de Heer *et al.,* in *Solid State Physics,* edited by H. Ehrenreich and D. Turnbull (Academic, New York, 1987), Vol. 40.
[16] A. Danon and A. Amirav, J. Phys. Chem. **93**, 5549 (1989).
[17] P. U. Andersson and J. B. C. Pettersson, Z. Phys. D **41**, 57 (1997).
[18] B. Bederson and L. J. Kieffer, Rev. Mod. Phys. **43**, 601 (1971).
[19] R. E. Collins *et al.,* Phys. Rev. A **3**, 1976 (1971).
[20] A. A. Agarkov *et al.* (to be published).
[21] K. D. Bonin and V. V. Kresin, *Electric-Dipole Polarizabilities of Atoms, Molecules and Clusters* (World Scientific, Singapore, 1997).
[22] L. D. Landau, E. M. Lifshitz, and L. P. Pitaevskii, *Electrodynamics of Continuous Media* (Pergamon, Oxford, 1984), 2nd ed., Sec. 3.
[23] C. E. Klots, J. Chem. Phys. **100**, 1035 (1994).
[24] A small source of error is the increased scattering length due to the electron spiraling in the magnetic field, coming primarily from the transverse thermal velocity at the cathode [P. O. Taylor *et al.,* Rev. Sci. Instrum. **45**, 538 (1974)]. A calculation shows that this may lead to an overestimate of the cluster size n by about 7%, corresponding to a change of about 3% in the cluster radius R.
[25] The deviation observed for energies above $\approx$2 eV is most likely due to the onset of a contribution from direct cluster fragmentation, similar to the behavior observed in the data for smaller alkali clusters [11]. Indeed, the heat of vaporization of sodium is 0.9 eV [*CRC Handbook of Chemistry and Physics* (CRC Press, Boca Raton, FL, 1988), 68th ed.], and a kinematic estimate shows that an electron, incoming with an energy of a few eV, can knock out a small fragment with an energy sufficient to remove the recoiling nanocluster from the collimated beam. This suggests direct, rather than evaporative, dissociation and raises interesting questions regarding the dynamics of electron-induced cluster fragmentation.
[26] C. Bréchignac *et al.,* Phys. Rev. B **47**, 2271 (1993).
[27] W. Bouwen *et al.,* Chem. Phys. Lett. **314**, 227 (1999).
[28] *Channeltron Electron Multiplier Handbook for Mass Spectrometry Applications* (Galileo Electro-Optics Corporation, Sturbridge, MA, 1991).
[29] C. F. Bohren and D. R. Huffman, *Absorption and Scattering of Light by Small Particles* (Wiley, New York, 1983).
[30] U. Kreibig and M. Vollmer, *Optical Properties of Metal Clusters* (Springer, Berlin, 1995).
[31] P. Markowicz *et al.,* Phys. Lett. A **236**, 543 (1997).
[32] M. Sanekata and I. Suzuka, Chem. Phys. Lett. **312**, 422 (1999).